Electrochimica Acta 79 (2012) 74–81

Contents lists available at SciVerse ScienceDirect

Electrochimica Acta

journal homepage: www.elsevier.com/locate/electacta

Arylated carbon nanotubes for biobatteries and biofuel cells

Krzysztof Stolarczyk[a], Dominika Łyp[a], Kamila Żelechowska[b], Jan F. Biernat[c], Jerzy Rogalski[d], Renata Bilewicz[a,*]

[a] Faculty of Chemistry, University of Warsaw, Pasteura 1, 02-093 Warsaw, Poland
[b] Faculty of Applied Physics and Mathematics, Gdansk University of Technology, Narutowicza 11/12, 80-233 Gdansk, Poland
[c] Department of Chemistry, Gdansk University of Technology Narutowicza 11/12, 80-233 Gdańsk, Poland
[d] Department of Biochemistry, Maria Curie Sklodowska University, Akademicka 19, 20-031 Lublin, Poland

ARTICLE INFO

Article history:
Received 5 March 2012
Received in revised form 31 May 2012
Accepted 17 June 2012
Available online 6 July 2012

Keywords:
Arylated carbon nanotubes
Bioelectrocatalysis
Oxygen reduction
Glucose oxidation
Biofuel cell
Laccase

ABSTRACT

Single-walled carbon nanotubes (SWCNTs) covalently phenylated, naphthylated or terphenylated were used for the construction of cathodes in a biobattery, and in a biofuel cell. Zn is the anode in the biobattery and single-walled carbon nanotubes are covalently modified with glucose oxidase/catalase (SWCNT-GOx/Cat) on the biofuel cell anode. The cell parameters were determined and the potentials of each of the electrodes under cell working conditions were simultaneously measured *vs.* the Ag/AgCl reference electrode. This allowed to evaluate the changes of potential under changing loads of the fuel cell or biobattery. A power density of ca. 1 mW/cm^2 was achieved using the biobattery with phenylated nanotubes at the cathode and the open circuit potential was 1.5 V. The fully enzymatic fuel cell studied had power density of 40 μW/cm^2 at 20 kΩ loading. The open circuit potential for the biofuel cell was 0.4 V. The power densities and working potentials are larger for the biobattery which is especially useful for testing novel cathodes.

1. Introduction

Biological fuel cells (BFCs) and biobatteries transform chemical energy into the electrical energy using enzymes as catalysts and natural compounds e.g. glucose or ethanol, as the fuels [1–9]. BFCs can utilize glucose and dioxygen dissolved in body fluids as fuel and oxidant, respectively, and could serve as power source for implanted devices such as, microvalves, drugs dispensers, pacemakers, and sensors [10]. The advantages of these biodevices are the specificity and selectivity of processes occurring at the enzymatically modified electrodes and the ability to operate at room temperature and at pH close to neutral. Biofuel cells that could also be constructed in membrane-less version can be easily miniaturized and, in addition, open construction allows the utilization of oxidant and fuel from the surrounding environment [4,7,11]. Important advantage of BFCs over conventional fuel cells is low cost of their components. Problems that still required to be solved are connected with the limited stability of the modified electrodes, transport limitations of the substrates and products of redox reactions, not efficient direct electron transfer due to large distance between the electrode surface and the active center of the enzyme, and limited number of enzyme molecules, that can be electrically connected with the electrode.

For the dioxygen bioelectrocatalytic reduction catalyzed by laccase or bilirubin oxidase, mediators are typically used to facilitate transfer of electrons between the electrode and the active site of the redox center, T1, hidden inside the protein in the hydrophobic pocket arranged by amino-acid residues [4,11]. Leaching of the mediators into the solution causes fast decrease of catalytic currents; on the other hand, side reactions with the components of the biocathode could cause the adverse effects of diffusing mediators. In our earlier reports, ABTS was chemically bonded to some extent preferentially to the sides or ends of single-walled carbon nanotubes (SWNTs) to eliminate leaching to the solution; in addition it significantly improved the catalytic efficiency of the modified cathode [12–15]. Carbon nanotubes (CNTs) can be easily modified non-covalently or by covalent bonding at the edges or defect sites and side-walls of the carbon nanotubes [16–23].

Minteer et al. [23] used multiwalled CNT modified at the ends with anthracene residues. The anthracene residue was bonded to phenolic hydroxylated carbon nanotubes forming ester groups. Carboxylates of phenols belong to so-called “active” esters that are known to be very sensitive to nucleophilic reactions, hence the stability of such modified carbon nanotubes may be quite limited.

The aryl moieties have been shown earlier to enter the hydrophobic pocket of T1 center of copper oxidoreductase

* Corresponding author. Tel.: +48 22 8220211x345; fax: +48 22 8224889.
E-mail address: bilewicz@chem.uw.edu.pl (R. Bilewicz).

0013-4686/$ – see front matter © 2012 Elsevier Ltd. All rights reserved.
http://dx.doi.org/10.1016/j.electacta.2012.06.050

facilitating direct electron transfer from the electrode [24]. Blanford et al. coupled anthracene residue to the surface of pyrolytic graphite electrode to improve the electrical contact with the enzyme active site and provide hydrophobic interaction that holds the enzyme at the electrode surface [24–26]. The modification required electrochemical generation of free radicals from anthracene diazonium salt. As shown by Sosna et al. [26] and Doppelt et al. [27], such modification led to the formation of a layer of branched anthracene structures, that are thicker than one molecule. This would explain the high oxygen catalytic currents obtained and the appearance of additional voltammetric peaks [26].

In our previous paper, we described SWCNT modified with anthraquinone or anthracene groups, either preferentially on the side or at the ends of the carbon nanotubes [28]. We compared these two types of modification in order to show that the redox properties of the group are not required for efficient electron transfer between the enzyme and the electrode. The electrodes were tested as cathodes in hybrid batteries. Laccase modified cathode nanostructured with arylated SWCNT were active towards dissolved dioxygen and the anode was Nafion-coated Zn wire covered by a protective film impermeable to dioxygen. Nanostructuring the electrode with arylated single-walled carbon nanotubes (SWCNTs) would transforms the 2D type of electrode surface modification into the 3D assembly connected electrically with the electrode. It allows significantly more laccase molecules to be connected with the electrode surface, leading as the result to evident increase of the catalytic oxygen reduction current. Fuel cell prototypes utilizing printed laccase–ABTS layer as the cathode and printed Zn layer as the anode have been constructed by Smolander et al. [29]. Under 2.2 kΩ load, the cell voltage of 0.6–0.8 V could be maintained for several days.

In a full biofuel cell glucose oxidase (GOx) is a most common anode biocatalyst. The main disadvantage of GOx based electrodes is that the hydrogen peroxide produced in the catalytic reaction can affect dioxygen catalytic reduction current [30]. To minimize this unfavorable effect, catalase together with GOx or dehydrogenases are frequently used instead [31–35].

Rincon and coworkers reported a fully enzymatic biofuel cell operating under a continuous flow – through regime [36]. A fungal laccase was used as air-breathing cathode, and maleate dehydrogenase (MDH) or alcohol dehydrogenase (ADH) coupled with poly-methylene green (poly-MG) were employed to modify the anode. An open circuit voltage (OCV) was 0.584 V for MDH-laccase, and 0.618 V for the ADH-laccase biofuel cells. Maximum power density was 20 $\mu W/cm^3$.

Ferapontova et al. constructed a biobattery based on the Zn anode and biocathode with laccases cross-linked onto graphite and microstructured graphitized carbon cloth (GCC) electrodes [37]. In this system the efficiency of the bioelectrocatalytic reduction of O_2 was enhanced by immobilizing laccases on the high-surface area GCC, due to the increased surface concentration of the laccase molecules properly oriented for the direct electron transfer reaction within the micro-structured electrode. An open circuit voltage (OCV) was 1.76 V. A maximum power density of the cell was 0.44 mW/cm^2 at the cell voltage of 0.5 V, pH 5. The biobattery with cross-linked stabilized laccases at GCC was able to power a 1.5 V domestic device for 38 days.

In the present paper, we compare the efficiencies of cathodes modified with SWCNT with phenyl, naphthyl and terphenyl moieties. The electrodes are tested as cathodes in hybrid biobattery and in a full biofuel cell. In the first case Zn wire covered with a Nafion film serves as the anode. In the second case, the anode is glassy carbon electrode covered with a mixture of single-walled carbon nanotubes (SWCNTs) bioconjugate with glucose oxidase and catalase, and multi-walled carbon nanotubes (MWCNTs) covalently modified with ferrocene.

2. Experimental

2.1. Materials and chemicals

Laccase *Cerrena unicolor* C-139 was obtained from the culture collection of the Regensberg University and deposited in the fungal collection of the Department of Biochemistry (Maria Curie-Sklodowska University, Poland) under the strain number 139. Laccase from the fermentor scale cultivation was obtained according to already reported procedure after ion exchange chromatography on DEAE-Sepharose (fast flow) [38] and lyophilized on Labconco (Kansas City, USA, FreeZone 12 Lyophiliser) in clear stoppering chambers. Laccase activity was measured spectrophotometrically with syringaldazine as the substrate [39]. The protein content was determined according to Bradford with bovine albumin as the standard [40]. The concentration of isolated and frozen (−18 °C) enzyme was *C*lacc = 178 $\mu g/cm^3$ and activity 186,000 $nkat/dm^3$. After lyophilizing, the laccase activity dissolved in 1 ml of water was 3,000,000 $nkat/dm^3$ and *C*lacc = 1.5 mg/cm^3.

Glucose oxidase and catalase, both from *Aspergillus niger* were purchased from Sigma (St Louis, USA), the inorganic reagents from POCh (Gliwice, Poland), and the organic reagents from Aldrich, were used without further purification. The GOx and Catalase activities were determined according to the procedures described previously [41,42]. Single-walled carbon nanotubes (>90%) purchased from CheapTubes.com (Brattleboro, USA) were washed with nitric acid/hydrochloric acid mixture before using for binding GOx and catalase. For arylation reaction SWCNT were used in the pristine form. For the preparation of MWCNTs with covalently bonded ferrocene the tubes from NANOCO Sp. z o.o. ul. Zagórska 159, 42-600 Tarnowskie Góry, Poland were used. Water was distilled and passed through Milli-Q purification system.

2.2. Apparatus

Thermogravimetric analysis (TGA) was done using Universal V4.3A TA Instrument. The measurements were carried out in argon atmosphere at a heating rate of 10°/min.

Raman spectra were collected using the Witec confocal Raman microscope system (Ulm, Germany) equipped with a fiber coupled Melles Griot (Carlsbad, CA) argon ion laser operating at 514.5 nm focused through a 60× objective. Collected light was dispersed through a triple monochromator (600 g/mm, 500 nm blaze angle) and detected with a thermoelectrically cooled (−60 °C) charge-coupled device. A small amount of carbon nanotubes in form of powder was placed on a microscope slide and covered with a coverslip. Laser power at the sample was approximately 5 mW.

Electrochemical experiments were done in three electrode arrangement with Ag/AgCl (KCl sat.) reference electrode, platinum foil as the counter electrode and glassy carbon electrode (GCE, BAS) as the working electrode with surface area of 0.071 cm^2. Cyclic voltammetry experiments were carried out using ECO Chemie Autolab potentiostat. All electrochemical measurements were done at 22 ± 2 °C. All current densities were calculated using geometrical area of the electrode.

2.3. Synthesis and characterization of arylated SWCNT

2.3.1. Purification of pristine SWCNT [43,44]

A suspension of pristine SWCNT in 4 N hydrochloric acid was sonicated at 50 °C for 4 h, the solid was collected by filtration and exhaustively washed with water until the pH of washings is close to 7. Then the solid was washed with methanol and dried in vacuum.

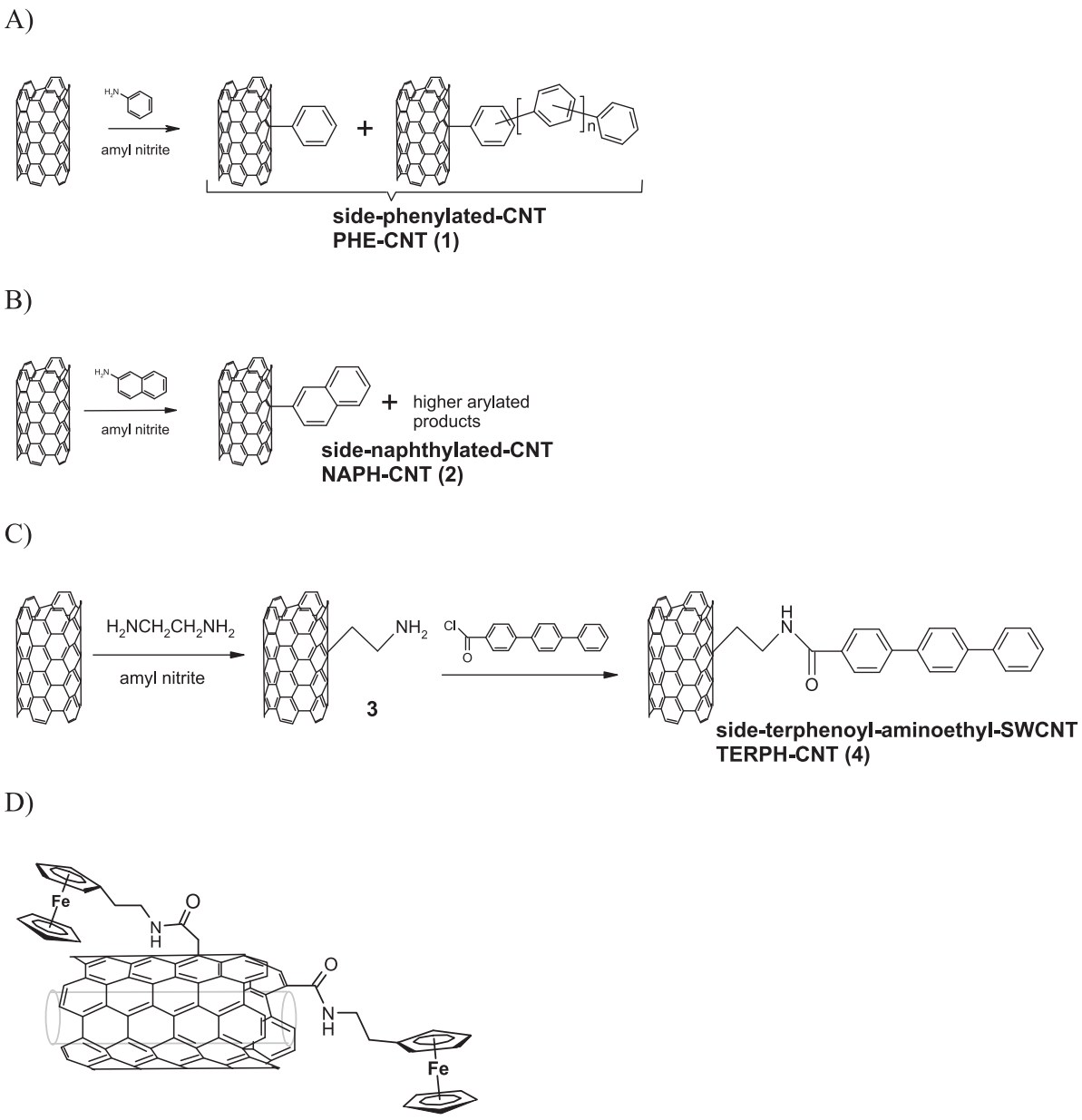

Fig. 1. (A) Phenylation of SWCNT on side walls: (PHE-CNT), (B) naphthylated SWCNT (2): side-naphthylated-CNT (NAPH-CNT), (C) N-terphenoyl-aminoethylated SWCNT (4) (TERPH-CNT), and (D) ferrocene modified carbon nanotubes (MWCNT-Fc).

2.3.2. Phenylation of SWCNT on side walls: side-PHE-CNTs (Fig. 1)

To a mixture of carbon nanotubes (CheapTubes; 50 mg, 4.125 mmol), aniline (0.484 ml, 5.2 mmol), chlorobenzene (5 ml) and acetonitrile (5 ml) sonicated for 15 min., amyl nitrite (0.69 ml, 5.2 mmol) was added. The mixture was sonicated at 65 °C for 6 h, diluted with DMF, sonicated for 5 min and centrifuged. This washing procedure was repeated 5 times, and then the mixture was washed with chlorobenzene, methanol, ethyl acetate, diluted acetic acid and acetone until the washings become clear and colorless. Finally the product was dried in vacuum. Free radical arylation of SWCNT proceeds not only on nanotube's carbon atoms, but also on aryl residues bonded to SWCNT on first stage of the reaction. The successive reaction is probably more efficient because aromatic residues are more reactive [24,26].

TGA: no solvent release was observed up to 200 °C. Maximum peaks at 350 °C with 4% weight loss and at 560 °C with 3% weight loss. Calculated molar ratio of phenyl residues directly or indirectly bonded to nanotube carbon atoms equals 0.012 (1.2×10^{-2}).

2.3.3. Naphthylated SWCNT (2): side-naphthylated-CNT, NAPH-CNT (Fig. 1B)

To a sonicated for 15 min mixture of pristine carbon nanotubes (40 mg, 3.3 mmol), 2-naphthylamine hydrochloride (936 mg, 5.2 mmol), pyridine (0.45 ml), *o*-dichlorobenzene (5 ml) and acetonitrile (5 ml), the amyl nitrite (0.72 ml, 5.2 mmol) was added. The mixture was sonicated and maintained at 65 °C for 6 h. Next the solid was collected, washed with DMF, toluene, ethyl acetate, acetonitrile, and finally with hot pyridine. After that the nanotubes were washed with methanol, 1 N HCl, again with methanol and chloroform and dried in vacuum.

As in the case of phenylated SWCNT the product contains not only naphthyl residues bonded to nanotubes, but also naphthylated naphthyl residues. TGA: 2% mass decrease was observed below 200 °C (maximum peak at 130 °C) due to removal of solvent, and 6% loss was found between 200 and 600 °C (maximum at 330 °C). The number of naphthyl residues directly or indirectly bonded to nanotube's carbon atoms equals 0.0061 (6.1×10^{-3}).

2.3.4. Aminoethylated SWCNT (1)

Aminoethylated SWCNTs (1) were obtained by a method similar to described by Price and coworkers [45]. To a sonicated for 10 min mixture of HCl treated SWCNT (300 mg, 24.75 mmol), ethylenediamine (2.08 ml, 31.2 mmol), 7 ml chlorobenzene and 7 ml acetonitrile, the isoamyl nitrite (2.7 ml, 15.6 mmol) was added. The mixture was heated and sonicated at 65 °C for 6 h in a sealed vessel. The cooled mixture was filtered on the membrane and the solid was dried in vacuum thoroughly washing procedure with methanol, and methylene chloride.

TGA: mass loss of 1% was found in the range up to 200 °C with maximum at 50 °C. In the range 200–600 °C 4% mass loss was found wit maximum at 310 °C. The calculated number of aminoethyl residues bonded to carbon atoms of nanotube's walls equals 1.4×10^{-2}.

2.3.5. N-terphenoyl-aminoethylated SWCNT (4); TERPH-CNT (Fig. 1C)

A mixture of terphenylcarboxylic acid (10 mg), thionyl chloride (1 ml) and a drop of dry pyridine was sonicated at 50 °C for 6 h. Then 2 ml of dry toluene was added and the excess of thionyl chloride and toluene was thoroughly removed under reduced pressure at 60 °C. To the residue diluted with pyridine (1.5 ml) aminoethyl-SWCNT-side (20 mg) was added and sonicated at 50 °C for 5 h. Then methanol was added, sonicated for 5 min and the mixture centrifuged at 10,000 × *g* min. The sediment was washed with methanol, chloroform, DMF, again with methanol and chloroform and dried under vacuum.

In this case oligo- or polymerization is not possible.

TGA: no solvent was released up to 200 °C. 11% mass loss was found between 200 and 600 °C with maximum at 385 °C. The calculated number of terphenoyl-aminoethyl residues bonded to carbon atoms of nanotube's walls equals 5×10^{-3}.

2.3.6. Ferrocene modified carbon nanotubes (MWCNT-Fc) (Fig. 1D)

Preparation of the MWCNT-Fc has been described earlier [15].

2.3.7. Glucose oxidase/catalase bioconjugate of carbon nanotubes (GCE/SWCNT-GOx/Cat)

Functionalized SWCNT containing amine as terminal groups (SWCNT–$(CH_2)_2$–NH_2) were used for the covalent immobilization of glucose oxidase and catalase. SWCNT–$(CH_2)_2$–NH_2 were sonicated for 4 h and activated with glutaraldehyde (5% in 0.1 M phosphate buffer pH 7.0) according to procedure published by Kamen and coworkers [46], in 1.5 ml Eppendorf tube by 8 h rotation in Rotator (Neolab, Heidelberg, Germany) at 10 rpm. Then the samples were centrifuged at 10,000 × *g* force for 8 min, washed by MilliQ water and centrifuged in the same as above conditions. The washing procedure was repeated 3 times. Next the GOx/catalase solution (1000 U/5000 U) with bovine albumine (added into 1 mg of protein in the mixture) was added to activated suspension of carbon nanotubes and allowed to react for 12 h under rotation at 10 rpm. The washing conditions of the obtained materials were as above.

2.4. Electrode modification procedures

GCE/SWCNT-aryl/laccase + Nafion electrode. Onto GCE surface 10 μl suspension of SWCNTs-aryl-side in ethanol (4 mg/ml) was dropped. After drying, 10 μl of enzyme/Nafion casting solution was pipetted onto the electrode and allowed to dry.

GCE/SWCNT-GOx/Cat/MWCNT-Fc electrode preparation – GCE surface was covered with mixture SWCNT-GOx/Cat and MWCNT-Fc by dropping a 10 μl suspension of nanotubes in ethanol (4 mg/ml) and allowed to dry.

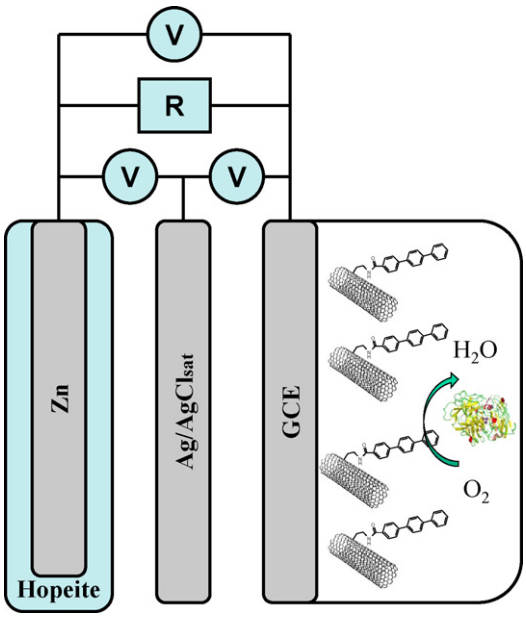

Fig. 2. Schematic representation of the biobattery circuit.

Laccase solution was prepared by dissolving 1 mg of enzyme in 0.64 ml McIlvaine buffer containing 0.2 M $NaNO_3$ (pH 5.2). 1% Nafion was prepared by dissolution of 5% Nafion in ethanol. Mixture of laccase and Nafion was prepared by mixing 50 μl of Nafion and 50 μl laccase solution. The biofuel cell parameters were examined in dioxygen saturated McIlvaine buffer solution (pH 5.2)/0.2 M $NaNO_3$ and in 0.2 M phosphate buffer (pH 7.1). Fig. 2 shows the configuration of the biobattery. Open circuit voltage (OCV) was measured in all experiments. The cell voltage (V_{cell}), the anode voltage (V_a), the cathode voltage (V_c) were measured under varying loadings in the range from 1 kΩ to 10 MΩ. To minimize the power loss caused by fuel depletion during the test, measurements under each load were restricted to 5 s. The anodes for the Zn–O_2 hybrid fuel cells (called further biobatteries) were zinc wires (0.25 mm diameter, Goodfellow) coated with a Nafion film by dipping in 0.5% Nafion solution in ethanol and dried for 5 min at ambient conditions. A hopeite layer was formed during the Zn electrode oxidation. The length of these electrodes were adjusted so as to obtain the same surface area as the cathode.

3. Results and discussion

3.1. Electrochemical studies

The reduction of dioxygen at a non-modified glassy carbon electrode (GCE) proceeds with large overpotential (ca. −0.6 V *vs.* Ag/AgCl) both in the absence and presence of laccase. In order to increase the efficiency of the system, the GCEs were structured with nanotubes covalently derivatized with phenyl-PHE-CNT (**1**), naphthyl-NAPH-CNT (**2**) and terphenyl-TERPH-CNT (**4**) moiety. We have recently shown that modification of electrodes with pristine SWCNT, SWCNT-anthraquinone and SWCNT-anthracene covalent combination, and laccase in a Nafion film leads to a decrease of the overpotential of dioxygen reduction. The onset of reduction current is at ca. +0.60 V *vs.* Ag/AgCl (+0.80 V *vs.* NHE) and current density measured at 0.2 V is 200 μA/cm^2 [14].

In the presence of covalently arylated SWCNT and laccase on the electrode, the dioxygen reduction wave appears at the same potential as on the pristine carbon nanotubes but the current density was higher (Fig. 3). The highest current density of dioxygen reduction was obtained for the electrodes structured with TERPH-CNT (**4**) and

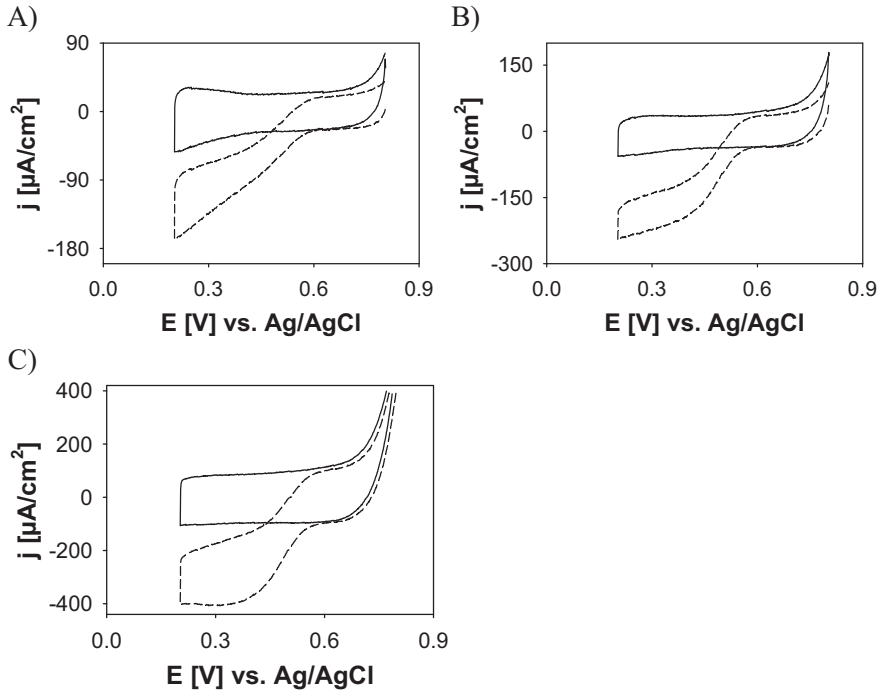

Fig. 3. Cyclic voltammograms recorded using electrodes modified with (A) PHE-CNT, (B) NAPH-CNT, (C) TERPH-CNT and covered with a Nafion film containing laccase, recorded in (—) deoxygenated and (– –) saturated with dioxygen solution of McIlvaine buffer + 0.2 M $NaNO_3$ (pH 5.2), scan rate 1 mV/s.

covered with Nafion film containing laccase (Table 1). The catalytic current density, equal to −388.3 μA/cm^2 was measured at 0.2 V.

The electrodes were tested in the biobattery. The power density–voltage and current density–voltage behavior of the biobattery were tested by applying different external loads. To minimize the power loss caused by fuel depletion during the test, measurements under each load were restricted to 5 s [47]. To enable monitoring the potential of each of the electrodes simultaneously to the measurement of the voltage of the full cell, the biobattery was tested in the three electrode arrangement: anode, cathode and reference electrode Ag/AgCl (KCl_{sat}). Variable loads, in the range from 1 kΩ to 10 MΩ, were applied between the anode and the cathode to determine the cell voltage (V_{cell}), the voltage between anode and reference electrode (V_a), and the voltage between cathode and reference electrode (V_c). During discharge of Zn anode in buffer solution a film of hopeite-phase $Zn_3(PO_4)_2{\cdot}4H_2O$ is deposited on its surface [29,37,48–53]. The film blocks the transport of oxygen to the Zn surface, thus enabling the necessary transport of Zn^{2+} while preventing Zn corrosion. Plots of power density *vs.* current density, cell voltage and *vs.* current density are presented in Fig. 4. Potentials of the anode and cathode *vs.* Ag/AgCl are plotted *vs.* current density flowing in the cell. The open circuit potential measured for all systems containing arylated SWCNT was ca. 1.5 V (Table 2). The best power density is achieved for the biofuel cell: anode–Zn/$Zn_3(PO_4)_2$, and cathode-modified PHE-CNT/laccase + Nafion. The maximal power density approaches 1145.7 μW/cm^2 at 900 mV and 10 kΩ loading.

The tri-electrode system is convenient for assessing the potential stability of each of the electrodes working in the cell. At large loadings, hence small current flow, the biocathode is stable, at high flows its potential decreases rapidly due to oxygen diffusion limitations. Up till 1500 μA/cm^2, the laccase based oxygen reduction controls the cathode potential.

Fig. 4B and C allows to compare the behavior of the biobattery where GCE is covered by PHE-CNT and a Nafion layer with and without laccase. It is proposed that in case of the ohmic loads in the range 10,000–10 kΩ the biobattery is operative while for lower resistances the cathode is working as a simple carbon nanotube modified electrode at potentials close to 0 V. At currents smaller than ca. 1500 μA/cm^2, the system is working as a biobattery, at higher currents the enzyme is not satisfactorily efficient and the cathodic process takes place at potentials close to 0 V *vs.* Ag/AgCl reference as in case of nanotube modified electrode. In all these cases the Zn anode potential is almost unaffected. Hence the tri-electrode monitoring system allows to follow the behavior of each of the electrodes under changing loading of the cell.

The electrodes with SWCNT-aryl-side were tested also in a full biofuel cell. In this case, the bioanode was constructed using multi-wall carbon nanotubes modified with ferrocene (MWCNT-Fc) and single wall carbon nanotubes modified with glucose oxidase and catalase (SWCNT-GOx/Cat). Linear dependence of ferrocene oxidation current at 0.4 V on glucose concentration was observed up till 160 mM of glucose (Fig. 5). H_2O_2 is not interfering in the process because it undergoes disproportionation to H_2O and O_2 catalyzed by catalase covalently bound to the same nanotubes. The buffer was changed to phosphate (pH 7.1) to be close to the biological pH conditions inside the body.

The bioanode was tested in the biofuel cell. The biofuel cell was constructed in three electrode system: anode, cathode and reference electrode Ag/AgCl (KCl_{sat}). Variable loads, in the range from 1 kΩ to 10 MΩ, were applied between the anode and the cathode

Table 1
Characteristics of electrodes covered with modified SWCNT-aryl-side and laccase/Nafion layer in deoxygenated and saturated with dioxygen in McIlvaine buffer solution (pH 5.2)/0.2 M $NaNO_3$.

SWCNT modified with:	j_{bcg} [μA/cm^2]	j_{cat} [μA/cm^2]	$j_{cat} - j_{bcg}$ [μA/cm^2]
PHE	−51.5 ± 2.4	−150.3 ± 23.9	−98.8 ± 21.1
NAPH	−51.0 ± 8.0	−241.2 ± 7.0	−190.2 ± 1.0
TERPH	−100.5 ± 9.8	−388.3 ± 21.0	−287.8 ± 11.2

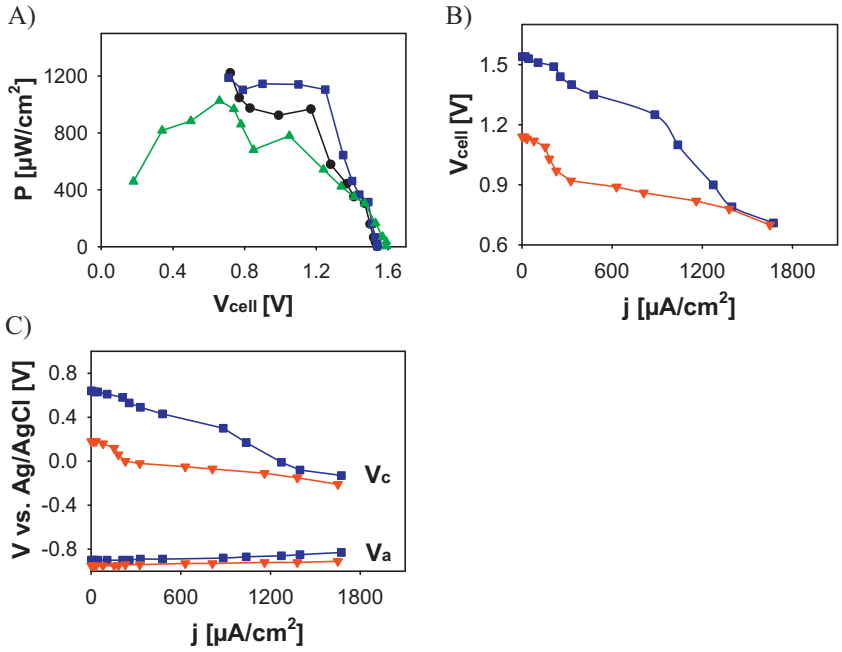

Fig. 4. (A) Dependence of power density on cell voltage for biobattery with cathodes modified with: (■) PHE-CNT (**1**), (●) NAPH-CNT (**2**), (▲) TERPH-CNT (**4**) and each of them covered with Nafion film containing laccase, anode: Zn electrode. Dependence of (B) biobattery voltage on current density; (C) cathode, V_c and anode, V_a potentials *vs.* Ag/AgCl (KCl_{sat}) on biobattery current density for the cathode modified with: PHE-CNT and covered with a Nafion film (■) with, and (▼) without laccase. Electrolyte: McIlvaine buffer with 0.2 M $NaNO_3$, pH 5.2.

Table 2
Characteristics of biobatteries and biofuel cells with three different cathodes. Biobattery electrolyte: McIlvaine buffer solution + 0.2 M $NaNO_3$ (pH 5.2), biofuel cell electrolyte: 0.2 M phosphate buffer solution (pH 7.1).

Anode	Cathode with laccase and SWCNTs modified on the walls with:	P_{max} [μW/cm²]	j [μA/cm²]	E [V]	R [kΩ]	E [OCV] [V]
Zn/hopeite-phase	PHE	1145.7	1272.9	0.90	10	1.54
	NAPH	968.1	827.4	1.17	20	1.54
	TERPH	1026.9	1555.9	0.66	6	1.59
Covered with SWCNT-GOx/Cat and MWCNT-Fc	PHE	40.7	169.7	0.24	20	0.41
	NAPH	18.1	113.2	0.16	20	0.37
	TERPH	11.1	39.6	0.28	100	0.35

to determine the cell voltage (V_{cell}), the voltage between anode and reference electrode (V_a), and between cathode and reference electrode (V_c). The plots of power and currents are presented in Fig. 6.

The open circuit potential measured for all systems containing arylated SWCNTs was ca. 0.4 V. The largest power density was obtained for the biofuel cell: consisting of a GCE modified with SWCNT-GOx/Cat and MWCNT-Fc as the anode, and the cathode modified with PHE-CNT/laccase in Nafion. The power density was 40 μW/cm² at 0.24 V under 20 kΩ load.

The parameters of the three biobatteries and three biofuel cells described in the present paper are compared in Table 2. The V_{cell} at 10 MΩ of the biobattery and the biofuel cell were monitored for 2 weeks (Fig. 6D). The V_{cell} for both of these devices were

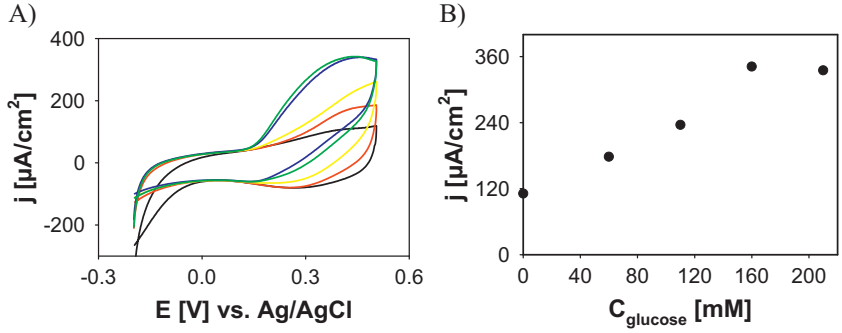

Fig. 5. (A) Cyclic voltammograms recorded using GCE electrodes modified with SWCNT-GOx/Cat and MWCNT-Fc for increasing concentration of glucose (—) 0 mM, (—) 60 mM, (—) 110 mM, (—) 160 mM, (—) 210 mM, scan rate 5 mV/s. (B) Dependence of current density of ferrocene oxidation on glucose concentration in oxygenated 0.2 M phosphate buffer solution (pH 7.1).

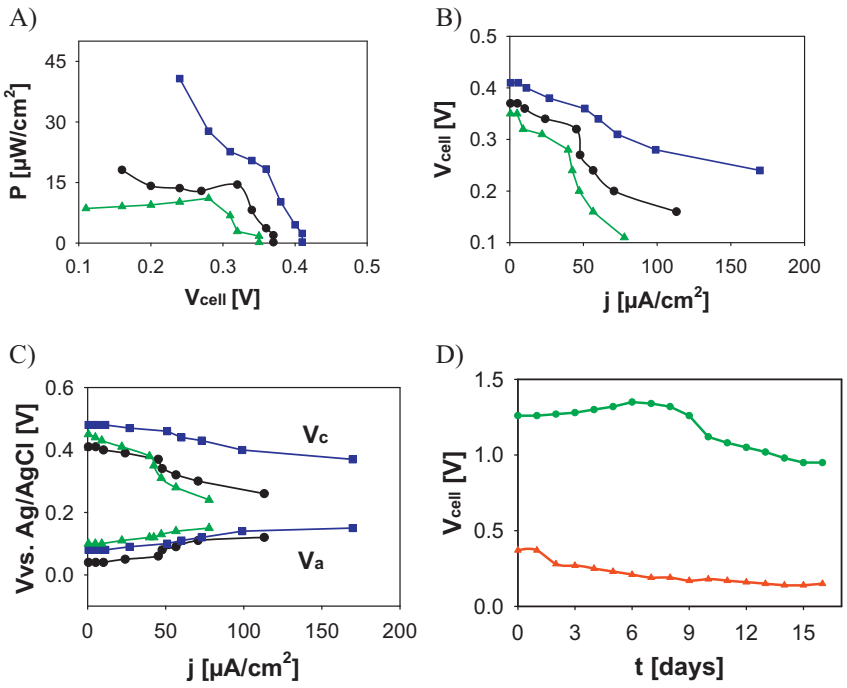

Fig. 6. Dependence of (A) power density and (B) cell voltage on current density for the biofuel cell with cathodes modified with: (■) PHE-CNT (**1**), (●) NAPH-CNT, (▲) TERPH-CNT and each of them covered with a Nafion film containing laccase and anode: SWCNT-GOx/Cat and MWCNT-Fc, (C) cathode, V_c and anode, V_a potentials (*vs.* sat. Ag/AgCl electrode) *vs.* biofuel cell current density, (D) dependence of V_{cell} on working time for the two systems studied: (●) biobattery: anode: $Zn/Zn_3(PO_4)_2$, cathode: GCE covered with PHE-CNTs and a film of Nafion containing laccase, (▲) biofuel cell: anode: SWCNT-GOx/Cat and MWCNT-Fc. Cathode: GCE covered with PHE-CNT and a film of Nafion containing laccase, electrolyte: 0.2 M phosphate buffer solution (pH 7.1) saturated with dioxygen and containing 0.21 M glucose.

satisfactorily stable – of course due to the very negative Zn anode potential the value of V_{cell} for the biobattery is much larger.

4. Conclusions

We compare the efficiencies of biobattery and enzymatic fuel cell that employ arylated carbon nanotubes to connect laccase electrically with the conducting support. We simultaneously monitor under external resistances: the cell power and the potential of each of the electrodes *vs.* Ag/AgCl reference electrode. This immediately shows which electrode determines the efficiency of the cell. The anodes used in the present work are more stable than the cathodes. The maximum power densities obtained for the hybrid biofuel cell with zinc wire anode and GCE cathode covered with PHE-CNT and laccase in Nafion film were ca. 1 mW/cm^2. The open cell voltage for the hybrid biobattery exceeds 1 V, hence it is higher than that of glucose–O_2 biobattery, due to negative value of Zn/Zn^{2+} redox potential ($E_0 = -0.76$ V *vs.* NHE [54]). This high cell voltage is shown to be stable for more than 2 weeks of continuous work of the cell. For the fully enzymatic biofuel cell with glucose oxidase/catalase bound covalently to SWCNT on the anode, the power density was 40 μW/cm^2 and the open circuit potential was 0.4 V. Biobatteries employing functionalized carbon nanotubes are demonstrated to be important alternative devices since they have much higher open circuit potentials and power outputs in comparison with the biofuel cells constructed so far. They are also a convenient choice for testing new types of biocathodes.

Acknowledgements

This work was supported by the Polish Ministry of Sciences and Higher Education, The National Center for Research and Development (NCBiR), grant NR05-0017-10/2010 (PBR-11) and by Faculty of Chemistry, University of Warsaw, grant BW 501/68-191210.

References

[1] A. Heller, Physical Chemistry Chemical Physics 6 (2004) 209.
[2] S.C. Barton, J. Gallaway, P. Atanassov, Chemical Reviews 104 (2004) 4867.
[3] B. Wang, Journal of Power Sources 152 (2005) 1.
[4] J.A. Cracknell, K.A. Vincent, F.A. Armstrong, Chemical Reviews 108 (2008) 2439.
[5] G.T.R. Palmore, H.H. Kim, Journal of Electroanalytical Chemistry 464 (1999) 110.
[6] R.A. Bullen, T.C. Arnot, J.B. Lakeman, F.C. Walsh, Biosensors and Bioelectronics 21 (2006) 2015.
[7] F.A. Armstrong, in: A. Wieckowski (Ed.), Fuel Cell Science: Theory, Fundamentals and Biocatalysis, John Wiley & Sons, Inc., Hoboken, NJ, 2010, pp. 237–257.
[8] M.H. Osman, A.A. Shah, F.C. Walsh, Biosensors and Bioelectronics 26 (2011) 3087.
[9] E. Nazaruk, S. Smoliński, M. Swatko-Ossor, G. Ginalska, J. Fiedurek, J. Rogalski, R. Bilewicz, Journal of Power Sources 183 (2008) 533.
[10] P. Cinquin, Ch. Gondran, F. Giroud, S. Mazabrard, A. Pellissier, F. Boucher, J.-P. Alcaraz, K. Gorgy, F. Lenouvel, S. Mathe, P. Porcu, S. Cosnier, PLoS One 5 (2010) e10476.
[11] R. Bilewicz, M. Opallo, in: A. Wieckowski (Ed.), Fuel Cell Science: Theory, Fundamentals and Biocatalysis, John Wiley & Sons, Inc., Hoboken, NJ, 2010, pp. 169–215.
[12] E. Nazaruk, K. Sadowska, K. Madrak, J.F. Biernat, J. Rogalski, R. Bilewicz, Electroanalysis 21 (2009) 507.
[13] R. Bilewicz, K. Stolarczyk, K. Sadowska, J. Rogalski, J.F. Biernat, ECS Transactions 19 (6) (2009) 27.
[14] K. Sadowska, K. Stolarczyk, J.F. Biernat, K.P. Roberts, J. Rogalski, R. Bilewicz, Bioelectrochemistry 80 (2010) 73.
[15] E. Nazaruk, K. Sadowska, J.F. Biernat, J. Rogalski, G. Ginalska, R. Bilewicz, Analytical and Bioanalytical Chemistry 398 (2010) 1651.
[16] A. Hirsch, Angewandte Chemie International Edition 41 (2002) 1853.
[17] C.A. Mitchell, J.I. Bahr, S. Arepalli, J.M. Tour, R. Krishnamoorti, Macromolecules 35 (2002) 8825.
[18] S. Banerjee, T. Hemraj-Benny, S.S. Wong, Advanced Materials 17 (2005) 17.
[19] K. Karnicka, K. Miecznikowski, B. Kowalewska, M. Skunik, M. Opallo, J. Rogalski, W. Schuhmann, P.J. Kulesza, Analytical Chemistry 80 (2008) 7643.
[20] M. Shim, N.W.S. Kam, R.J. Chen, Y. Li, H. Dai, Nano Letters 2 (2002) 285.
[21] R.J. Chen, S. Bangsaruntip, K.A. Drouvalakis, N.W.S. Kam, M. Shim, Y. Li, W. Kim, P.J. Utz, H. Dai, Proceedings of the National Academy of Sciences of the United States of America 100 (2003) 4984.
[22] M. Jönsson, K. Szot, J. Niedziolka, J. Rogalski, K. Karnicka, P. Kulesza, M. Opallo, Journal of Nanoscience and Nanotechnology 9 (2009) 2346.
[23] M.T. Meredith, M. Minson, D. Hickey, K. Artyushkova, D.T. Glatzhofer, S.D. Minteer, ACS Catalysis 1 (2011) 1683.
[24] Ch.F. Blanford, R.S. Heath, F.A. Armstrong, Chemical Communications (2007) 1710.

[25] C.E. Banks, G.G. Wildgoose, C.G.R. Heald, R.G. Compton, Journal of the Iranian Chemical Society 2 (2005) 60.
[26] M. Sosna, J.-M. Chretien, J.D. Kilburn, P.N. Bartlett, Physical Chemistry Chemical Physics 12 (2010) 10018.
[27] P. Doppelt, G. Hallais, J. Pinson, F. Podvorica, S. Verneyre, Chemistry of Materials 19 (2007) 4570.
[28] K. Stolarczyk, M. Sepelowska, D. Lyp, K. Zelechowska, J.F. Biernat, J. Rogalski, K.D. Farmer, K.N. Roberts, R. Bilewicz, Bioelectrochemistry (2011), http://dx.doi.org/10.1016/j.bioelechem.2011.10.001.
[29] M. Smolander, H. Boer, M. Valkiainen, R. Roozeman, M. Bergelin, J.-E. Eriksson, X.-C. Zhang, A. Koivula, L. Viikari, Enzyme and Microbial Technology 432 (2008) 93.
[30] P. Scodeller, R. Carballo, R. Szamocki, L. Levin, F. Forchiassin, E.J. Calvo, Journal of the American Chemical Society 322 (2010) 11132.
[31] A. Zebda, C. Gondran, A. Le Goff, M. Holzinger, P. Cinquin, S. Cosnier, Nature Communications 2 (2011) 1.
[32] O. Yehezkeli, R. Tel-Vered, S. Raichlin, I. Willner, ACS Nano 5 (2011) 2385.
[33] D. Wen, L. Deng, M. Zhou, S. Guo, L. Shang, G. Xu, S. Dong, Biosensors and Bioelectronics 25 (2010) 1544.
[34] T. Miyake, M. Oike, S. Yoshino, Y. Yatagawa, K. Haneda, H. Kaji, M. Nishizawa, Chemical Physics Letters 480 (2009) 123.
[35] F. Tasca, W. Harreither, R. Ludwig, J.J. Gooding, L. Gorton, Analytical Chemistry 83 (2011) 3042.
[36] R.A. Rincon, C. Lau, H.R. Luckarift, K.E. Garcia, E. Adkins, G.R. Johnson, P. Atanassov, Biosensors and Bioelectronics 27 (2011) 132.
[37] U.B. Jensen, S. Lörcher, M. Vagin, J. Chevallier, S. Shipovskov, O. Koroleva, F. Besenbacher, E.E. Ferapontova, Electrochimica Acta 62 (2012) 218.
[38] G. Janusz, Ph.D. Thesis, UMCS, Lublin, 2005, p. 222.
[39] A. Leonowicz, K. Grzywnowicz, Enzyme and Microbial Technology 3 (1981) 55.
[40] M.M. Bradford, Analytical Biochemistry 72 (1976) 248.
[41] J. Rogalski, J. Fiedurek, J. Szczodrak, K. Kapusta, A. Leonowicz, Enzyme and Microbial Technology 10 (1988) 508.
[42] J. Rogalski, J. Fiedurek, A. Gromada, Acta Microbiologica Polonica 47 (1998) 31.
[43] J. Zhang, H. Zou, Q. Qing, Y. Yang, Q. Li, Z. Liu, X. Guo, Z. Du, Journal of Physical Chemistry B 107 (2003) 3712.
[44] A.R. Harutyunyan, B.K. Pradhan, J.P. Chang, G.G. Chen, P.C. Eklund, Journal of Physical Chemistry B 106 (2002) 8671.
[45] B.K. Price, J.M. Tour, Journal of the American Chemical Society 128 (2006) 12899.
[46] D.A. Lappi, F.E. Stolzenbach, N.O. Kaplan, M.D. Kamen, Biochemical and Biophysical Research Communications 69 (1976) 878.
[47] J. Ge, R. Schirhagl, R.N. Zare, Journal of Chemical Education 88 (2011) 1283.
[48] A. Zloczewska, M. Jönsson-Niedziolka, J. Rogalski, M. Opallo, Electrochimica Acta 56 (2011) 3947.
[49] A. Heller, Analytical and Bioanalytical Chemistry 385 (2006) 469.
[50] W. Shin, J. Lee, Y. Kim, H. Steinfink, A. Heller, Journal of the American Chemical Society 127 (2005) 14590.
[51] W. Nogala, A. Celebanska, G. Wittstock, M. Opallo, Fuel Cells 10 (2010) 1157.
[52] K. Szot, W. Nogala, J. Niedziolka-Jönsson, M. Jönsson-Niedziolka, F. Marken, J. Rogalski, C. Nunes Kirchner, G. Wittstock, M. Opallo, Electrochimica Acta 54 (2009) 4620.
[53] J. Martinez-Ortiz, R. Flores, R. Vazquez-Duhalt, Biosensors and Bioelectronics 26 (2011) 2626.
[54] A.J. Bard, L.R. Faulkner, Electrochemical Methods: Fundamentals and Applications, 2nd ed., Wiley, New York, 2001.